STUDIA UBB CHEMIA, LXVII, 2, 2022 (p. 175-191)
(RECOMMENDED CITATION)
DOI:10.24193/subbchem.2022.2.11

CHITOSAN-COATED SILICA NANOPARTICLES DEPOSITED BY ELECTROPHORESIS ON ZINC FOR ANTICORROSIVE PROTECTION

ÁRPÁD FERENC SZŐKE[a], CLAUDINE FILIÂTRE[b], LIANA MARIA MUREȘAN[c*]

ABSTRACT. Silica nanoparticles were covered with a thin layer of chitosan to obtain a positive surface charge. The resulting silica/chitosan nanoparticles were characterized using zeta potential and particle size analysis before being electrophoretically deposited on zinc substrates to obtain an anticorrosive coating. The uniformity of the resulting layers was studied by optical and scanning electron microscopy. The anticorrosive properties were determined using potentiodynamic polarization and electrochemical impedance spectroscopy. Results show non-uniform deposits of nanoparticles. Nevertheless, the electrochemical measurements point to a relatively significant corrosion inhibition efficiency of the coating (*ca.* 60-80%) which increases with the time of deposition.

Keywords: *chitosan, silica nanoparticles, electrophoretic deposition, zinc, corrosion*

INTRODUCTION

Silica nanoparticles are versatile materials [1] with several important advantages such as biocompatibility [2], a simple production process [3], as well as controlled particle size and particle size distribution [4]. Special attention is accorded to porous silica nanoparticles, as in addition to the particle size, the pore size and size distribution can also be tailored for specific applications [5], resulting in the availability of a wide array of nano-, meso- and microporous silica nanoparticles.

---

[a] *Babeş-Bolyai University, Faculty of Chemistry and Chemical Engineering, Department of Chemistry and Chemical Engineering of the Hungarian Line*

[b] *Institut UTINAM, UMR-CNRS 6213, Université de Bourgogne Franche-Comté, Besançon, France*

[c] *Babeş-Bolyai University, Faculty of Chemistry and Chemical Engineering, Department of Chemical Engineering*

* *Corresponding author: liana.muresan@ubbcluj.ro*

As such, they have been considered for several different applications, such as drug [6] and enzyme [7] carriers, anticorrosive additives [8], adsorption agents, etc. Although these studies mainly focus on porous silica as a possible carrier [9], compact nanoparticles have also been tested as additives in polymeric coatings, usually incorporated into polymeric matrices where they can improve the structural stability of the coatings [8].

Silica surfaces have a negative charge under most pH conditions [10], which is neutralized only by strongly acidic environments. As such, the application of silica nanoparticles on a negatively charged zinc substrate is not possible. To circumvent this problem, silica nanoparticles can be coated with a positively charged polymer, like chitosan. Chitosan (Chit) is composed of randomly distributed β-linked D-glucosamine and N-acetyl-D-glucosamine [11]. As the amine groups can be protonated partially or completely, chitosan becomes soluble in acidic environments. Bridging the positive charges in linear chitosan using covalent or ionic crosslinking agents can significantly affect structural stability, water permeability and solubility [12, 13, 14]. Due to its versatility and ease of structural modification, chitosan is considered a possible eco-friendly alternative for several applications in a wide range of industries such as agriculture [15], medicine [16], anticorrosive protection [17] and water purification [18]. As chitosan possesses antimicrobial properties, it has also been considered to counter microbial corrosion [19]. Previous studies show that thin chitosan layers show good adhesion to zinc surfaces, which can be explained by the presence of trace amounts of oxidized groups on the metal surface [20]. The swelling properties of thin chitosan layers hinder shielding properties. As such, native chitosan cannot form effective anticorrosive coatings [14].

It was assumed that chitosan and silica nanoparticles can form strong electrostatic bonds [21] with a thin chitosan layer surrounding the silica core. This should result in a silica/chitosan nanoparticle with a positive surface charge.

In this context, chitosan-coated silica nanoparticles were produced from commercially available SiO_2 nanoparticles and low molecular weight (lmw) chitosan. These were deposited on zinc substrates to obtain a protective barrier with increased anticorrosive properties. To the best of our knowledge, no previous studies were published regarding films formed by electrophoretic deposition of chitosan-coated silica nanoparticles on zinc substrates.

The nanoparticles were characterized using total organic carbon (TOC) content, particle size and zeta potential analysis. The uniformity of the coatings was studied using optical and scanning electron microscopy. Their anticorrosive properties were determined using potentiodynamic polarization and electrochemical impedance spectroscopy techniques.

RESULTS AND DISCUSSION

Adsorption of chitosan on the silica nanoparticles

TOC analysis shows a decrease in the carbon content in the chitosan solutions when SiO_2 nanoparticles are added to them (Figure 1). This difference was attributed to chitosan adsorption on the surface of the silica cores.

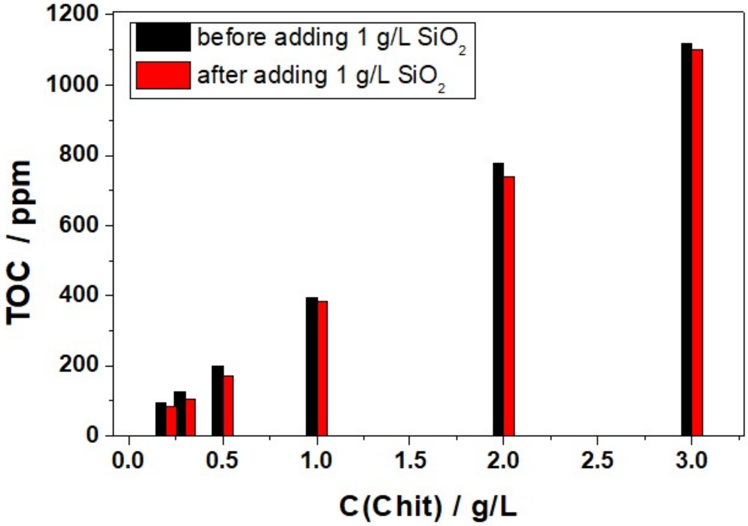

Figure 1. Total organic carbon content analysis of low molecular weight chitosan solutions with varying concentrations before (**black**) and after (**red**) adding 1g/L Si nanoparticles.

The zeta potential of the chitosan-coated silica nanoparticles was determined for different chitosan concentrations. It can be observed, that initially, an increased amount of chitosan resulted in increased zeta potential; which finally reached a plateau at 50-60 mV, when 1 g/L chitosan was added to 1 g/L SiO_2 (Figure 2).

The diameter of the chitosan/SiO_2 nanoparticles was measured in function of chitosan concentration. Composite particle size is equal to about 500 nm for chitosan concentration below 500 mg/g(SiO_2) (Figure 3). Particles are positively charged and the plateau of adsorption is not reached. For higher chitosan concentration, particle size increased. This may be due to polymer adsorption on a few particles.

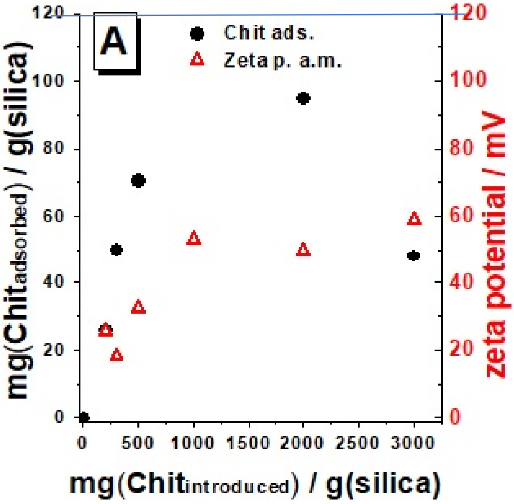

Figure 2. Amount of chitosan adsorbed on SiO_2 (●) and zeta potential determined with auto-mode (Δ) as a function of the added amount of chitosan. Experimental conditions: low molecular weight chitosan, 1 g/L silica, 25 °C, pH 4.

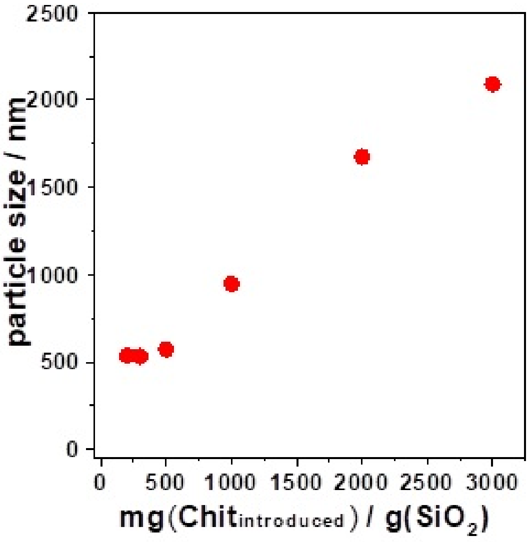

Figure 3. Particle size of chitosan-coated silica nanoparticles as a function of chitosan added to the SiO_2 dispersion. Experimental conditions: low molecular weight chitosan, 1 g/L silica, 25 °C, pH 4

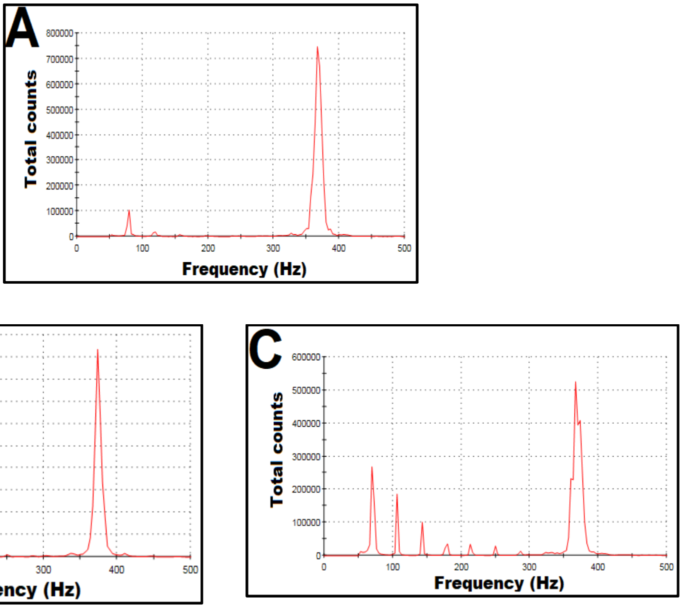

Figure 4. Frequency plots of 500 mg(Chit$_{introduced}$)/g(SiO_2) system immediately after agitation (**A**), after 30 minutes of sedimentation (**B**) and after 60 minutes of sedimentation (**C**).

To determine the temporal stability, a chitosan-coated silica nanoparticle dispersion was chosen with minimal particle size (*i.e.* 500 mg chitosan added to 1 g/L silica nanoparticle dispersion). Frequency dependence plots were determined at room temperature at different time intervals after the agitation of the mixtures (Figure 4). These show a relatively monodisperse system initially, which gradually becomes more polydisperse after 30 and 60 minutes of sedimentation, respectively. As such, to obtain a more uniform coating, dispersions should be freshly used.

Optical microscopy of the coated zinc plates

Visual inspection of the coated zinc substrates pointed to a non-uniform surface coverage, which was verified using different optical methods.

Optical microscopy confirmed our initial observation, showing a non-uniform coating of nanoparticles (observable as dark patches on the micrographs). 30 minutes of electrophoretic deposition resulted in only small patches of nanoparticles on the zinc surface (Figure 5 B). An increased time of 90 minutes of electrophoretic deposition increased the amount of deposited particles significantly; however, the uniformity of the coating did not improve significantly (Figure 5 C) [22].

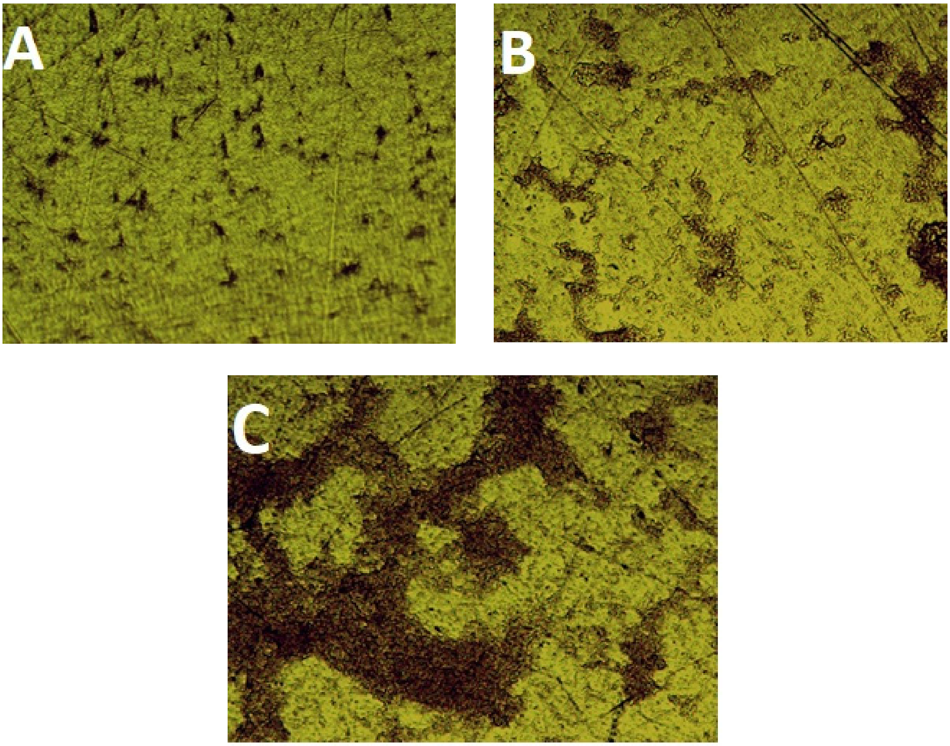

Figure 5. Optical microscopy images of a bare, polished Zn plate (**A**), and zinc substrates coated by electrophoretic deposition for 30 minutes (**B**) and 90 minutes (**C**), respectively. Magnification: **20X**.

Scanning electron microscopy

The scanning electron microscopy study further corroborates the visual and optical microscopy inspection, with a non-uniform coating regardless of ED duration (Figure 6). It should be noted, that the number of nanoparticles and coverage are significantly better when the particles were deposited for 90 minutes.

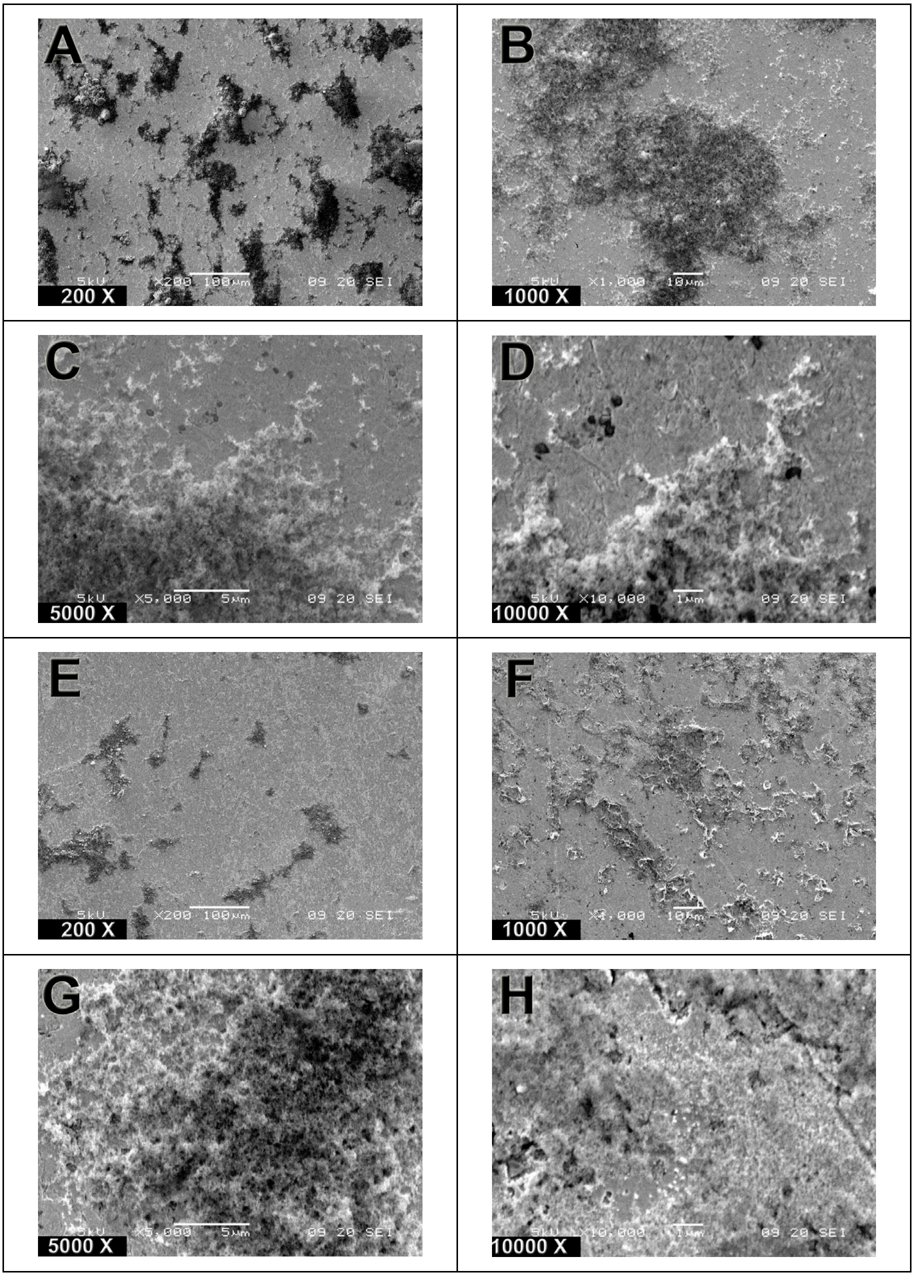

Figure 6. SEM images of coated zinc substrates after 30 minutes (A, B, C, D) and after 90 minutes (E, F, G, H) of ED at increasing magnifications.

Previous studies attributed the good adhesion of dip-coated chitosan layers on zinc to the presence of oxide and hydroxide traces on the metal surface [20]. In our case, it was theorized that the nanoparticles were initially deposited more efficiently at sites where surface defects (irregularity or oxidation) were present. The deposited nanoparticles electrostatically repulsed further nanoparticles, resulting in the uneven coverage [23].

Electrochemical analysis

The polarization resistance of the coated samples was improved compared to bare zinc, as seen from the Nyquist impedance spectra (Figure 7). The fitted equivalent electrical circuit proposed for uncoated Zn was $R(Q_1R_1)$, with R representing the resistance of the Na_2SO_4 electrolyte solution used for electrochemical measurements, R_1 representing the charge transfer resistance and Q_1 is a constant phase element for a non-ideal system, characterizing the double layer capacity through the following equation:

$$C = R^{\frac{1-n}{n}} Q^{\frac{1}{n}}, \text{ [24]},$$

where n is a coefficient representing the depressed feature of the capacitive loop.

Similar to our previous studies of chitosan-coated zinc samples, an $R(Q_1R_1(LR_2))$ equivalent circuit showed the best fit for the nanoparticle-coated zinc. In this case, the additional LR_2 pair could be attributed to the resistance of the coating and the swelling properties of chitosan [14]. The similar curves and values of the charge transfer resistance for the reproduced systems (Table 1, *ca.* 3500 Ωcm^2 for 30 minutes and *ca.* 6000 Ωcm^2 for 90 minutes ED) demonstrate a good reproducibility, despite the uneven coating observed by optical studies. It can also be observed that the resistance value attributed to the coating itself greatly increased when 90 minutes of ED was used. This is due to the increased amount of nanoparticles on the zinc surface, as observed in the optical analysis.

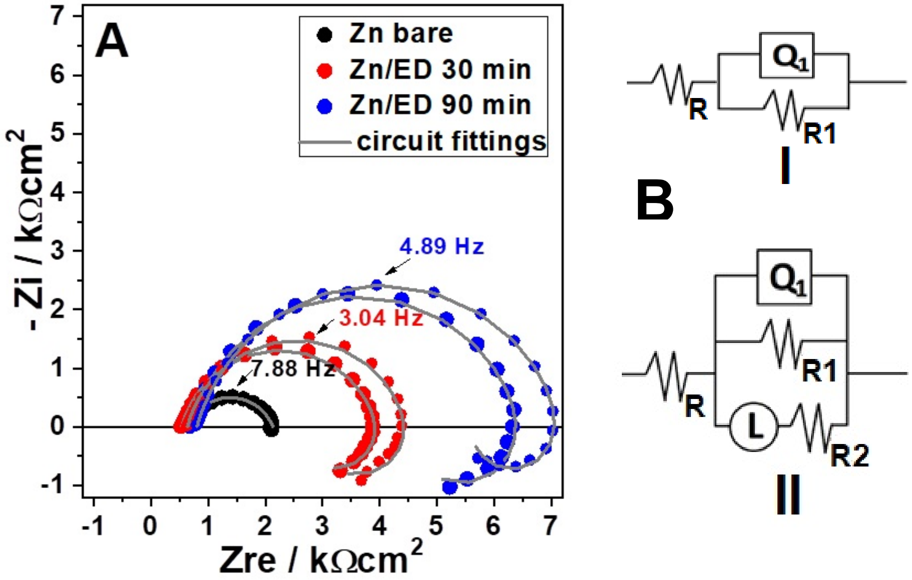

Figure 7. Nyquist impedance spectra of bare Zn and Chit/SiO$_2$ coated Zn (A), and fitted equivalent electric circuits (B) for the bare zinc substrate (B - I) and the nanoparticle-coated zinc substrate (B - II).
Experimental conditions: 0.2 g/L Na$_2$SO$_4$ solution (pH 5.0); frequency interval, 10 kHz – 10 mHz; OCP, 60 minutes.

Table 1. Electrochemical parameters obtained from the Nyquist impedance spectra [22].

Samples	R (Ωcm^2)	Q$_1$ (μSs^n)	R$_1$ (Ωcm^2)	L (kH)	R$_2$ (Ωcm^2)	Chi^2
Zn	508	40.0	1460	-	-	0.38 X 10^{-3}
Zn/ED 30 min_1	539	17.8	3419	124	4707	0.72 X 10^{-3}
Zn/ED 30 min_2	638	19.5	3846	109	4983	1.22 X 10^{-3}
Zn/ED 90 min_1	696	15.9	5798	176	10910	0.38 X 10^{-3}
Zn/ED 90 min_2	804	9.50	6428	95	18860	0.22 X 10^{-3}

1 and_2 notations represent the reproduction of the systems in the same conditions

Polarization curves (Figure 8) corroborate EIS results with decreased current densities for the coated samples prepared with 30 and 90 minutes of ED [22]. The inhibition efficiency values determined from the polarization curves show an anticorrosive effect of *ca.* 60% for 30 minutes of ED and *ca.* 75% for 90 minutes of ED (Table 2.).

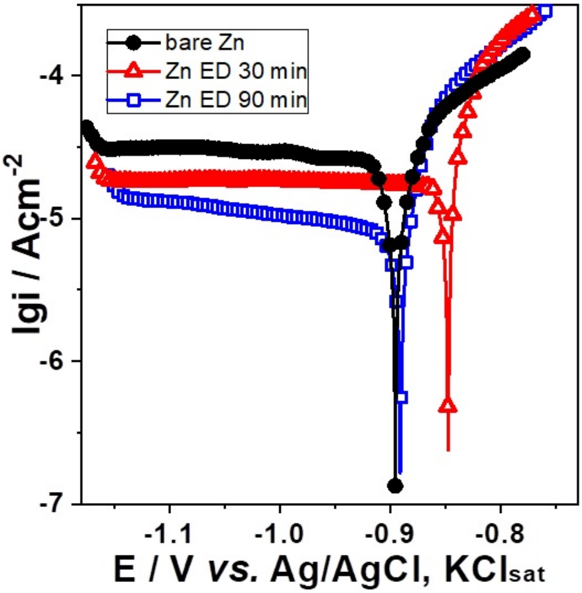

Figure 8. Semi-logarithmic polarization curves (current density *vs*. potential) of bare Zn (●), Zn/ED 30 min (□) and Zn/ED 90 min (▲) systems
Experimental conditions: 0.2 g/L Na_2SO_4 solution, scan rate, 0.166 mV/s, OCP, 60 minutes.

Table 2. Electrochemical parameters of various coated zinc samples determined from the polarization curves [22].

Sample	E_{corr} (V)	b_c (V/dec)	b_a (V/dec)	i_{corr} (μA / cm^2)	IE (%)
Zn bare	-0.893	-	0.188	41.56	-
Zn/ED 30 min	-0.847	-	0.133	15.00	63.91
Zn/ED 90 min	-0.891	0.949	0.165	9.60	76.90

As a non-destructive method, electrochemical impedance spectroscopy was used to study the short- and long-term effects of exposure to a corrosive environment (Figure 9 and 10, Table 3).

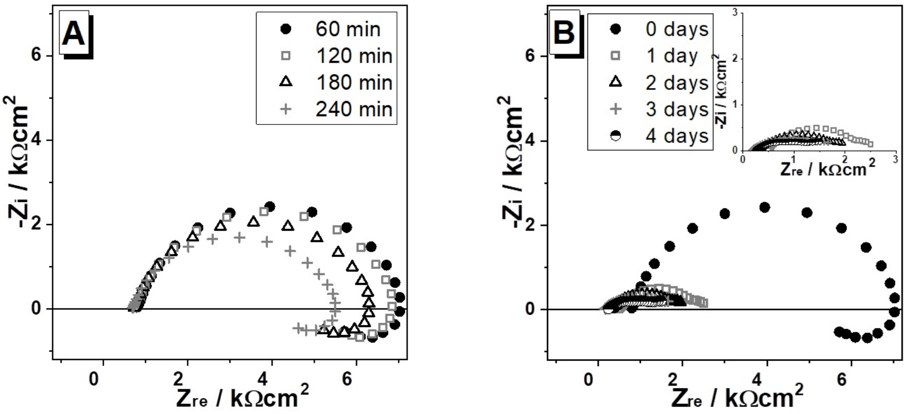

Figure 10. Nyquist impedance spectra of Zn/ED 90 min during short- (A) and long-term (B) exposure to a corrosive medium. Experimental conditions: 0.2 g/L aqueous Na_2SO_4 solution (pH = 5), frequency interval, 10 kHz - 10 mHz, OCP, 60 minutes (day 0), 10 minutes (days 1-4).

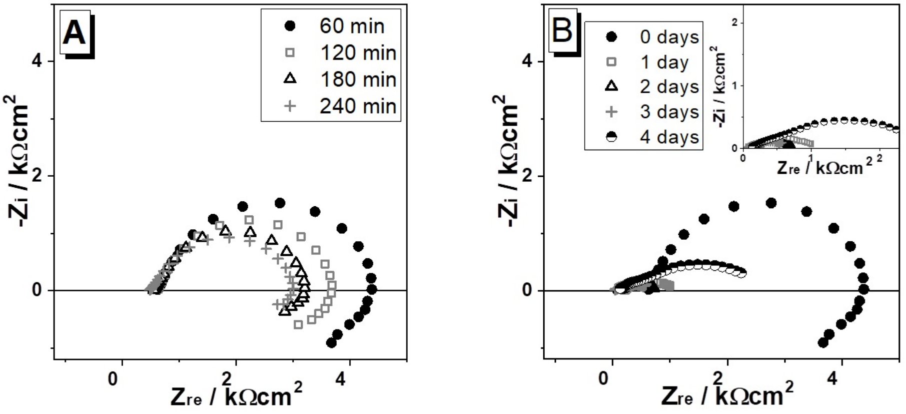

Figure 9. Nyquist impedance spectra of Zn/ED 30 min during short- (A) and long-term (B) exposure to a corrosive medium. Experimental conditions: 0.2 g/L aqueous Na_2SO_4 solution (pH = 5), frequency interval, 10 kHz - 10 mHz, OCP, 60 minutes (day 0), 10 minutes (days 1-4).

Table 3. Rp value change of studied samples during short- and long-term EIS studies.

Sample	unit	60 min	120 min	180 min	240 min	1 day	2 days	3 days	4 days
Zn/ED 30 min	kΩcm^2	3.77	3.09	2.66	2.51	0.79	0.60	0.53	2.11
Zn/ED 90 min	kΩcm^2	6.23	6.07	5.57	4.84	2.01	1.64	1.49	1.25

For both 30 and 90 minutes of ED, the diameter of the Nyquist curves (which represents the polarization resistance) decreased each hour after exposure, pointing to diminishing anticorrosive protection. In the case of samples prepared with 30 minutes of ED, the initial Rp value of 3.77 kΩcm^2 dropped to 2.51 kΩcm^2 after 4 hours. For 90 minutes of ED, the initial value of 6.23 kΩcm^2 dropped to 4.84 kΩcm^2 in the same time period, underlining that the diminishing effect is less pronounced for substrates coated with 90 minutes of ED. Similarly, the Rp values of corresponding curves were always significantly higher (around twofold) in the case of the longer deposition time.

The study of long-term exposure also shows a gradual polarization resistance decrease, however, in the case of the sample coated with 30 minutes of ED, the polarization resistance actually increased after 4 days (from 0.53 to 2.11 kΩcm^2) probably due to the deposition of corrosion products on the zinc surface and its partial blocking.

CONCLUSIONS

Chitosan-coated silica nanoparticles were successfully prepared by adsorption of the polymer on commercial silica nanoparticles. The so-prepared nanoparticles obtained a significant positive charge in slightly acidic conditions, offering a possibility to be electrophoretically deposited on zinc.

The optical study shows an uneven deposition of nanoparticles on the zinc surface. Electrochemical studies point to significant coverage of the zinc surface, resulting in anticorrosive activity, as proved by both polarization and impedance spectroscopy measurements. This effect is improved when a longer period of deposition is used.

The significant anticorrosive effect of the layers, in contrast with their uniformity probably occurred due to nanoparticle deposition at surface defects.

EXPERIMENTAL SECTION

Materials and methods

37% HCl from VWR was diluted to dissolve the low molecular weight chitosan. The pH was adjusted using NaOH from Riedel-de-Haen. 99.9% Sodium chloride and 99.6% isopropanol were obtained from VWR. Low molecular weight (50000-190000 Da) chitosan (lmw Chit) was purchased from Aldrich, Aerosil 200 silica nanoparticles from Degussa. Distilled water was prepared with a Millipore synergy UV water purifier.

The pH was measured using a pH meter from Mettler Toledo with a combined glass electrode.

The zinc plates were obtained from Bronzker BT and cut into 2x5 cm pieces. The surface of zinc was smoothed by polishing with different types of abrasive paper (2000, 4000, 5000), until mirror-aspect. Any residual powder from the polishing process was removed by 2x5 minutes of ultrasonication in isopropanol. Finally, the zinc plates were rinsed with 0.1 M HCl and distilled water to remove any remaining oxide or hydroxide from the surface [20, 22], and coated immediately.

Adsorption of chitosan on silica, TOC analysis

The adsorption of the chitosan on the silica nanoparticles was determined using TOC analysis on a **T**otal **O**rganic **C**arbon content analyzer from Shimadzu.

A series of lmw Chit (0.02, 0.03, 0.05, 0.1, 0.2, 0.3 w/w%) solutions were prepared by dissolving chitosan in 0.1 M HCl. Following an initial TOC analysis to be used as a reference, the pH of the solutions was set to 4 (favoring adsorption) and silica nanoparticles were added to reach a concentration of 1 g/L. To adequately cover the silica nanoparticles with chitosan, it is preferred that the two materials have an opposite surface charge. Chitosan molecules get protonated in acidic conditions and their surface charge becomes more positive with a lower pH. In contrast, silica surfaces have a negative surface charge, which becomes neutral only in strongly acidic environments. As such, a pH level of 4 was chosen, where chitosan dissolves effectively through protonation, while the silica nanoparticles should still have a negative surface charge.

The agglomerates in the silica nanoparticles were dispersed by 5 minutes of ultrasound treatment. The mixture was then left overnight under agitation, so the chitosan was adsorbed on the nanoparticles. The suspensions were then centrifuged at a speed of 10000 rpm, for 10 minutes; parameters were determined with equation (1) [22].

$$v = \frac{2\,(\rho_p - \rho_L)\,Gg\,a_p^2}{9\,\eta} \qquad (1)$$

Where:

v - sedimentation speed (m/s)
ρ_P - density of the particles (kg/m^3)
ρ_L - density of the liquid (kg/m^3)
g - gravitational constant (m/s^2)
*η - viscosity (Pa*s)*
a_P – particle radius (m)
G – number that multiplies g because of the rotation speed

$$G = \frac{R\omega^2}{g}$$

The resulting chitosan solution was studied by TOC analysis. The results were compared to the reference solutions before some of the dissolved chitosan was adsorbed on the silica nanoparticles.

Zeta potential and particle size analysis

The study was conducted on a Zetasizer from Malvern Panalytical. The same series of solutions were used to determine the zeta potential and particle size of the Chitosan/SiO_2 nanoparticles.

Electrophoretic deposition

Based on previous experience and results obtained for adsorption and zeta potential, an optimized recipe was used consisting of 200 mL solution containing 0.04025 w/w% Chit (or 402,5 mg Chit$_{introduced}$/gSi), 1 g/L silica nanoparticles, 0.365 M HCl (to dissolve the chitosan), NaOH (to set the pH levels to the desired value of 4) and 0.3 M NaCl. A minimum amount of 30 minutes (under constant stirring) was given for the adsorption to take place [22].

An undivided three-electrode cell was put together with a platinum-plate as the counter electrode, a Ag/AgCl reference electrode and the polished Zn plate as the working electrode.

The electrophoretic deposition (ED) was conducted at an applied potential of -1.5 V under constant, slow magnetic stirring. If we observed a large amount of bubble formation, the voltage was decreased to -1.4 V. After 30 minutes, or 90 minutes, respectively, the suspension was replaced with distilled water and, for a few minutes, a potential of -5 V was applied to stabilize the coated system [25].

Optical microscopy and SEM analysis

Following ED, the samples were dried. To verify the dispersion of the nanoparticles and the effectiveness of the coating, optical microscopy (with a Moticam microscope camera, 5 MP and an Olympus IC 20 microscope objective) and scanning electron microscopy (JEOL 5510LV) were conducted on the coated samples.

Electrochemical study

Electrochemical measurements were performed using a PARSTAT-2273 computer-controlled potentiostat (Princeton Applied Research, United Kingdom). An undivided electrochemical cell containing the coated zinc sample (1 cm^2 surface area) as the working electrode, a platinum wire as the counter (Type P131 Radiometer, France) and a Ag/AgCl,KCl$_{sat}$ reference electrode (Radiometer, France) were connected to the potentiostat. All experiments were carried out at room temperature (25 °C) [22].

Electrochemical impedance spectroscopy (EIS) measurements were conducted in a 0.2 g/L aqueous Na_2SO_4 (pH = 5) solution as the electrolyte. It should be noted that this pH value differs from the ideal pH for the coated nanoparticle formation (which is pH 4). The reason for this is that previous studies point to chitosan being relatively stable at these conditions [14], as well as the fact that naturally occurring corrosive environments often have similar pH values.

The open circuit potential (OCP) was measured for 60 minutes before the initial EIS measurements. In the case of subsequent EIS measurements (after exposures to the corrosive medium between 1 hour and 4 days), the open circuit potential was stable after 10 minutes.

The frequency interval of the measurements was 10^4 Hz - 10^{-2} Hz at open circuit potential (OCP). The experimental spectra were fitted with different electrical equivalent circuits by using the ZSimpWin 3.21 software.

Potentiodynamic polarization curves were recorded with a scan rate of 10 mV/min, in a potential range of OCP ± 200 mV *vs*. Ag/AgCl, KCl$_{sat}$. The inhibition efficiency was calculated using the formula (2):

$$\text{IE}(\%) = 100 \cdot \frac{i_{corr}^{0} - i_{corr}}{i_{corr}^{0}} \quad (2)$$

ACKNOWLEDGEMENTS

Arpad Szőke would like to thank the Erasmus+ mobility program for his stage at UFR des Sciences et Techniques, University of Franche-Comté, Besancon, France and Dr. Nicolas Rouge for the SEM measurements.

REFERENCES

1. P. G. Jeelani; P. Mulay; R. Venkat; C. Ramalingam; *Silicon-Neth.*, **2020**, *12*, 1337–1354
2. O. Esim; S. Kurbanoglu; A. Savaser; S. A. Ozkan; Y. Ozkan, Nanomaterials for Drug Delivery Systems. In *New Developments in Nanosensors for Pharmaceutical Analysis*, S. A. Ozkan, A. Shah Eds.; Academic Press, **2019**, Chapter 9, pp. 273-301
3. L. P. Singh; S. K. Bhattacharyya; R. Kumar; G. Mishra; U. Sharma; G. Singh; S. Ahalawat; *Adv. Colloid Interfac.*, **2014**, *214*, 17-37
4. S. Nagappan; A. Mohan; A. M. Thomas; J.-M. Yoo; N. Eid; I. Chung; B. Ameduri; C.-S. Ha; *RSC Adv.*, **2021**, *11*, 2194-2201
5. E. Albert; N. Cotolan; N. Nagy; Gy. Sáfrán; G. Szabó; L.-M. Mureşan; Z. Hórvölgyi; *Microp. Mesopor. Mat.*, **2015**, *206*, 102-113
6. N.-T. Nguyen-Thi; L. P. P. Tran; N. T. T. Le; M.-T. Cao; T.-N. Tran; N. T. Nguyen; C. H. Nguyen; D.-H. Nguyen; V. T. Than; Q. T. Le; N. Q. Trun; *Processes*, **2019**, *7(11)*, 805
7. B. Szokol; G. Hornyánszki; J. Nagy; *Stud. U. Babes-Bol. Che.,* **2019**, *LXIV 2 Tom I*, 69-78
8. L. V. Mora; S. Naik; S. Paul; R. Dawson; A. Neville; R. Barker; *Surf. Coat. Tech.*, **2017**, *324*, 368-375
9. M. Yeganeh; M. Omidi; S. H. H. Mortazavi; A. Etemad; M. H. Nazari; S. M. Marashi; Application of mesoporous silica as the nanocontainer of corrosion inhibitor. In *Micro and Nano Technologies, Corrosion Protection at the Nanoscale*, S. Rajendran, T. A. N. H. Nguyen, S. Kakooei, M. Yeganeh, Y. Li, Eds.; Elsevier, **2020**, Chapter 15, pp. 275-294
10. S. H. Behrens; D. G. Grier; *J. Chem. Phys.,* **2001**, *115*, 6716-6721
11. R. C. Cheung; T. B. Ng; J. H. Wong; W. Y. Chan; *Mar. drugs*, **2015**, *13(8)*, 5156–5186
12. J. Berger; M. Reist; J. M. Mayer; O. Felt; N. A. Peppas; R. Gurny; *Eur. J. Pharm. Biopharm.,* **2004***, 57,* 19–34
13. L. Y. Pozzo; T. F. Conceição; A. Spinelli; N. Scharnagl; A.T.N. Pires; *Carbohyd. Polym.*, **2018**, *181,* 71–77
14. Á. F. Szőke; G. S. Szabó; Z. Hórvölgyi; E. Albert; L. Gaina; L. M. Muresan; *Carbohyd. Polym.*, **2019**, *215*, 63-72
15. S. Bandara; H. Du; L. Carson; D. Bradford; R. Kommalapati; *Nanomaterials-Basel,* **2020**, *10(10)*, 1903
16. D. Zhao; S. Yu; B. Sun; S. Gao; S. Guo; K. Zhao; *Polymers-Basel*, **2018**, *10(4)*, 462
17. Á. F. Szőke; G. Szabó; Z. Simó; Z. Hórvölgyi; E. Albert; A. G. Végh; L. Zimányi; L. M. Muresan; *Eur. Polym. J.,* **2019***, 118*, 205-212
18. A. J. Al-Manhel; A. R. S. Al-Hilphy; A. K. Niamah; *J. Saudi Soc. Agric. Sci.,* **2018**, *17(2),* 186-190

19. P. A. Rasheed; R. P. Pandey; K. A. Jabbar; A. Samara; A. M. Abdullah, A. M.; K. A. Mahmoud; *Materials,* **2020***, 13(11),* 2484
20. Á. F. Szőke; G. S. Szabó; Z. Hórvölgyi; E. Albert; A. G. Végh; L. Zimányi; L. M. Muresan; *Int. J. Biol. Macromol*., **2020**, *142*, 423-431
21. M. Dabóczi; E. Albert; E. Agócs; M. Kabai-Faix; Z. Hórvölgyi; *Carbohyd. Polym.*, **2015**, *136*, 137–145
22. Á. F. Szőke; Polymer-modified surfaces for electroanalytical applications and anticorrosive protection, PhD Thesis, **2019**
23. C. Dange-Delbaere; C. C. Buron; M. Euvrard; C. Filiatre; *Colloid. Surface. A*, **2016**, *493*, 1-8
24. M. N. Kakaei; J. Neshati; A. R. Rezaierod; *Prot. Met. Phys. Chem. Surf.,* **2018**, *54*, 548–556
25. C. Pignolet; C. Filiatre ; A. Foissy; *Langmuir,* **2008**, *24(18),* 10181-10186.